Vacuum Ultraviolet–Induced Photochemical Nitriding of Polyolefin Surfaces

F. Truica-Marasescu, M. R. Wertheimer

Groupe de Couches Minces (GCM), Department of Engineering Physics, Ecole Polytechnique, Montreal, QC H3C 3A7, Canada

Received 24 July 2003; accepted 26 September 2003

ABSTRACT: Film samples of two very pure polyolefins, low-density polyethylene (LDPE) and biaxially oriented polypropylene (BOPP), were surface-modified by vacuum ultraviolet (VUV) photochemistry in low-pressure ammonia. The influence of experimental conditions such as wavelength and intensity (photon flux) of the VUV radiation, ammonia pressure, and treatment duration, as well as the mechanisms involved in the surface modification were discussed. Changes in the surface energy and chemistry were investigated using suitable techniques like contact angle goniometry (surface energy) measurements, X-ray photoelectron spectroscopy (XPS), attenuated total reflectance infrared spectroscopy, and time-of-flight secondary ion mass spectroscopy. We show that chemically bonded nitrogen concentrations [N], up to 25%, can be achieved on the polymer surfaces by VUV photochemistry, and that N is predominantly bonded as amine groups, thus leading to an important increase in the surface energy of treated samples. Finally, XPS, surface energy measurements, and atomic force microscopy were used to characterize possible degradation of the polymer surfaces during the VUV treatments.
© 2004 Wiley Periodicals, Inc. J Appl Polym Sci 91: 3886–3898, 2004

Key words: photochemistry; polyethylene; polypropylene; surface energy; surface chemistry

INTRODUCTION

Many applications of polymers require modified surface properties, either uniformly on the whole surface or on restricted areas. A variety of methods can be used for modifying polymer surfaces, several based on "cold" plasma treatments at low pressure[1] or at atmospheric pressure.[2,3] The resulting changes in surface composition, morphology, and surface energy can improve wettability, adhesive bonding, biocompatibility, and many other surface-related properties. A particular component of low-pressure plasmas, that is, short-wavelength [vacuum ultraviolet (VUV), $\lambda < 200$ nm] radiation, is believed to play an important role in the near-surface chemistry of plasma-treated polymers[4,5]; hydrocarbon polymers display a very strong absorption band below 160 nm that originates from electronic excitation of carbon–carbon and carbon–hydrogen σ bonds.[6–9] This absorption results in bond scission and in the formation of free radicals such as alkyl or/and allyl,[9–11] which are then able to undergo further reactions with other free radicals, including ones in the neighboring gas phase,[12,13] thereby forming either new chemical species (functionalities) bonded onto the polymer surface or a three-dimensional network (i.e., crosslinking).[9,11,14] One possible advantage of VUV photochemistry over its plasma counterparts may be that a more specific surface chemistry is achieved using monochromatic radiation because of more specific and selective (photo) chemistry both on the solid surface and in the gas phase.[15]

An important concern in the polymer film–converting industry is treatment-induced material degradation and the production of so-called low molecular weight oxidized material (LMWOM).[2,3] LMWOM generation on polyolefin surfaces was previously reported to result from high-energy corona treatment,[2,3] low-pressure plasma treatment in oxygen,[13] and ultraviolet/ozone treatment.[16] LMWOM mainly consists of oxidized oligomers, which are believed to be generated as reaction products during cleavage of C—C bonds of polymer chains, concurrent with oxidation processes.[2,3,13] These light products are characterized by a higher mobility than that of intact polymer chains (because of their low molecular mass), and they thus tend to agglomerate on treated surfaces as "nodules," probably attributable to favorable surface energies.[3] Because they are easily removed from the surface by rinsing with polar solvents (e.g., water), their presence can pose problems in certain applications requiring good adhesion, for example.

Correspondence to: M. Wertheimer.
Contract grant sponsor: Natural Sciences and Engineering Research Council of Canada (NSERC).
Contract grant sponsor: Ministère de l'Éducation of Quebec.

© 2004 Wiley Periodicals, Inc.

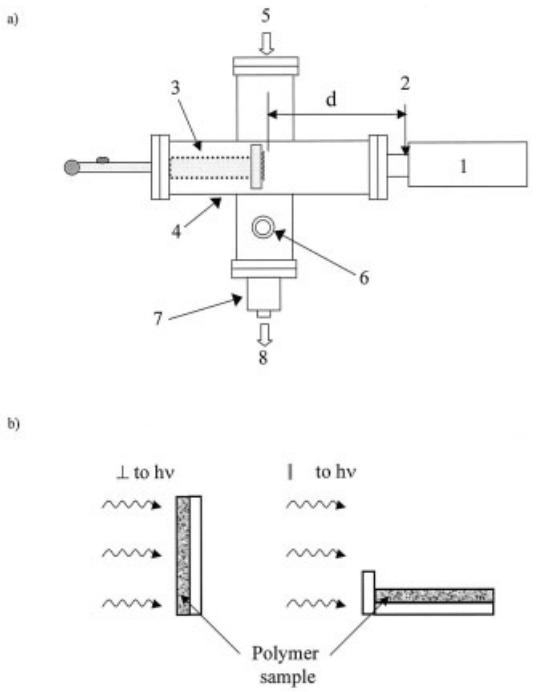

Figure 1 (a) Experimental setup: (1) VUV lamp, (2) MgF_2 window, (3) movable sample holder, (4) stainless-steel vacuum chamber, (5) gas inlet, (6) pressure gauge, (7) butterfly valve, (8) vacuum pumps; (b) sample orientation with respect to the VUV photon flux: perpendicular (⊥) and parallel (∥) to hν.

In the present article, we extend our previous work[12] on VUV photochemical modification of polyolefin surfaces in ammonia; we report the influence of experimental parameters such as VUV radiation wavelength and intensity, gas pressure, and treatment duration on the extent of surface physicochemical modification. We discuss possible mechanisms involved, the formation of new chemical species and the resulting surface energy increase, and surface material degradation leading to "LMWOM." We use the same term LMWOM, as in the literature, even though light products created during VUV photochemistry in ammonia certainly have different chemical compositions and molecular mass distributions than those created by the above-mentioned oxidizing treatments.

EXPERIMENTAL 1

Polymer characteristics

The polyethylene used in this study was a melt-extruded, low-density (LDPE) film (35 μm thick), supplied by the Chevron Phillips Company, and contained no additives. The base resin had a weight-average molecular weight of 1.2×10^5 and a polydisperity index of 5.3.

The second polymer was a melt-extruded, isotactic, biaxially oriented polypropylene (BOPP) film (50 μm thick) graciously provided by the 3M Co. (St. Paul, MN). The base resin contained approximately 200 ppm of an inorganic acid scavenger and about 1000 ppm of a high molecular weight hindered phenolic antioxidant. It was characterized by a weight-average molecular weight of 3.6×10^5 and a polydispersity index of 4. The additives contained in our BOPP appeared not to be surface active because they were not detected either by X-ray photoelectron spectroscopy (XPS) or by time-of-flight secondary ion mass spectroscopy (ToF-SIMS) analysis of either untreated or treated BOPP films. Furthermore, no bound oxygen or nitrogen was detected by XPS or ToF-SIMS on the untreated surface of either film.

Using the method of Owens et al.,[17,18] the total surface energy γ_s of the untreated polymers was estimated to be 27 ± 1 mN/m (or dynes/cm) for BOPP and 28 ± 1 mN/m for LDPE.

VUV treatments

The experimental setup used for the VUV treatments is presented schematically in Figure 1(a). Before the experiments, the sample chamber (4) was evacuated by a turbomolecular pump (8) to a base pressure of about 5×10^{-6} Torr ($\sim 7 \times 10^{-4}$ Pa) and then filled with pure ammonia (electronic grade) at low pressure, typically between 0.05 Torr (6.7 Pa) and 0.5 Torr (66.7 Pa), controlled by a butterfly valve (7). The VUV sources (1) used for this study were commercial resonant or excimer lamps with MgF_2 windows (2, cutoff wavelength, $\lambda_c = 112$ nm, from Resonance Ltd., Barrie ON, Canada), based on low-pressure radiofrequency (RF) discharges in noble gases. The characteristics of these lamps are summarized in Table I and in Figure 2(b–d). The polymer samples (4×4-cm squares) were mounted on a stainless-steel sample holder (3), which could move axially within the treatment chamber, over a maximal distance of 10 cm. This allowed us to vary the sample distance d with respect to the lamp window, and thereby also the VUV power density arriving at the polymer surface, according to the Beer–Lambert law:

$$I_s = \int_{\lambda} \frac{I_0(\lambda)}{d^2} \exp(-K(\lambda)pd)\, d\lambda \ (W/cm^2) \qquad (1)$$

TABLE I
VUV Lamps Used and Their Characteristics Measured Under High Vacuum at a Frontal Distance, d = 6 cm

Lamp type	Peak wavelength (nm)	Power density (mW/cm^2)	Photon flux ($\times 10^{14}$) (ph cm^{-2} s^{-1})
Kr line	123.6	1.06	7
D_2Ar continuum	110–170	0.78	6
Xe excimer	172	0.26	2

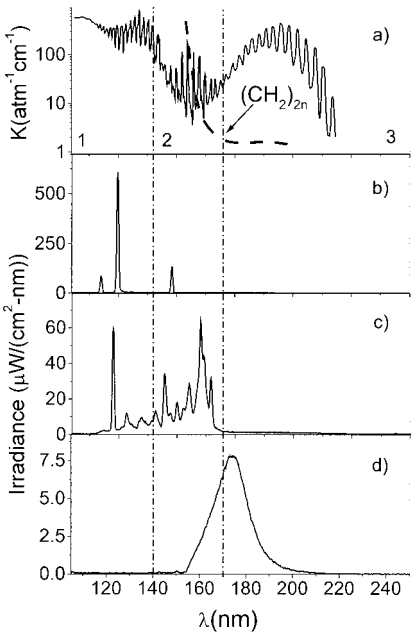

Figure 2 (a) Absorption coefficients: of ammonia[18] (continuous line); polyolefin[6] optical density (dashed line). Intensities and spectral distributions of the VUV radiation emitted by the (b) Kr lamp; (c) D_2Ar lamp; and (d) Xe excimer lamp.

where I_0 and I_s are the intensities at the MgF_2 window and at the polymer surface, respectively; K is the absorption coefficient of ammonia (NH_3)[19] [see Fig 2(a)] (in cm^{-1}/atm^{-1}); p is the NH_3 pressure; and d is the distance between the sample and the MgF_2 window. The energy density E_d was calculated using the following formula:

$$E_d = I_s t \quad (J/cm^2) \tag{2}$$

where t is the treatment duration (typically between 2 and 70 min). Figure 1(b) shows two different sample orientations used during VUV irradiation experiments; the purpose of these will be explained and discussed later.

Surface analysis

The physicochemical effects of treatments on the polyolefin surfaces were investigated using a combination of analytical techniques. After each treatment the surface energy γ_s of the samples was determined by contact angle measurements (typically, within 1 h after the treatment), using several probe liquids, that is, water, glycerol, formamide, ethylene glycol, and tricresyl phosphate. Using the method of Owens/et al.,[17,18] we calculated the polar (γ_s^p) and dispersive (γ_s^d) components of the polymer surface energy. X-ray photoelectron spectroscopy (XPS) analyses were performed in a VG Escalab 3MkII system, using nonmonochromatic Mg–K_α radiation, no later than 24 h after the treatment (we noticed no change in the chemical composition of the treated samples during this time). Spectra were acquired at a takeoff angle (TOA) = 0°, normal to the surface, and possible surface-charging effects were corrected by referencing all peaks with respect to the C—C and C—H component of the carbon (Cls) peak, at binding energy (BE) = 285.0 eV. Standard deviations of N/C and O/C atomic ratios were ±0.03; this value indicates the combined reproducibility of both treatment and of the XPS technique.

Samples were also analyzed by Fourier transform infrared spectroscopy, in the attenuated total reflectance mode (ATR-FTIR), at 45° incidence. For this, we used a germanium crystal, a trapezoid (50 × 20 × 2 mm) with a 45° facet angle (Single Pass Trapezoid Plate, from Harrick Scientific Corp.) in a Digilab FTS-3000 Excalibur Series spectrometer equipped with a deuterated triglycine sulfate (DTGS) detector. The background was determined with the Ge prism and then subtracted from the spectra of both untreated and treated samples.

Static ToF-SIMS analysis was carried out (typically within 1 h after the treatment) with a ToF-SIMS IV (from ION-TOF GmbH, Germany). The primary ion beam (15 keV $^{69}Ga^+$), in the so-called high current bunched mode, was rastered over an area of 200 × 200 μm, keeping the total dose below 10^{12} ions/cm^2 (so-called static conditions).

A Digital Instruments Dimension 3100 atomic force microscope (AFM; Digital Instruments, Santa Barbara, CA) was used to examine the topographical features of the polypropylene surface before and after treatment. All AFM images were acquired in the tapping mode at a scan rate of 1 Hz, using etched silicon cantilever probes having a radius of curvature between 5 and 10 nm and a resonant frequency of about 217 kHz.

To study the creation of LMWOM on VUV-treated surfaces of both polymers, surface energy, XPS, and AFM data were obtained in conjunction with rinsing of the samples: immediately after the treatment, the sample was agitated in a bath of deionized water for 1 min, then dried under a jet of pure, dry nitrogen, followed by a 10-min exposure to ambient air. After this, contact angle measurements were performed under the same conditions used for measurements on unwashed samples.

RESULTS AND DISCUSSION

VUV treatments in ammonia

From spectroscopic measurements, performed using a NIST-calibrated VUV/visible spectrophotometer (Acton Research Corp. VM 502, nominal resolution 0.4 nm), the irradiance and spectral characteristics of our

VUV sources were established with care. These results, measured under high vacuum at $d = 6$ cm, are presented in Figure 2(b)–(d) and summarized in Table I. The Kr resonant lamp was seen to be nearly monochromatic, with about 75% of the nominal power density (~ 1.06 mW/cm^2) at $\lambda = 123.6$ nm. The D_2Ar lamp emits a polychromatic radiation ($\lambda < 170$ nm), similar to the emission of hydrogen, or Ar/H_2 plasma,[4,5,20] which includes the Lyman α-line (Ly α; $\lambda = 121.5$ nm), representing about 10% of the total VUV radiation power, and the molecular Lyman and Werner bands. The Xe_2^* excimer lamp exhibits a 16-nm half-width optical emission, centered at 172 nm. For the purpose of initiating photochemical reactions, this lamp can be considered nearly "monochromatic".[15]

Gaseous ammonia absorbs strongly in the 112 to 220-nm spectral range [see Fig. 2(a) given that its bond energy is approximately D_0 (H—NH_2) = 4.4 eV, the absorption of energetic VUV photons ($h\nu > 6.2$ eV) will lead to photodissociation of the NH_3 molecule, followed by a redistribution of the excess energy to the resulting fragments.[19] The spectral region $112 < \lambda < 140$ nm (region 1 in Fig. 2) is characterized by a high absorption coefficient of about 1.3×10^5 atm^{-1} cm^{-1} (integrated value) and about 1.2×10^4 atm^{-1} cm^{-1} at $\lambda = 123.6$ nm, attributed to the transitions $\tilde{C}'\ A_1'$, $\tilde{D}'A_2''$ and $\tilde{E}'\ A_2''$–$\tilde{X}'\ A_1$ (ground state) of ammonia. In the region $140 < \lambda < 170$ nm (region 2 in Fig. 2), the absorption attributed to the $\tilde{B}'\ E''$–$\tilde{X}'\ A_1$ transition is lower ($\sim 1.2 \times 10^4$ atm^{-1} cm^{-1} integrated value). Finally, in the third region in Figure 2 ($170 < \lambda < 220$ nm), the absorption is comparable with that in the first region ($K = 0.6 \times 10^5$ atm^{-1} cm^{-1} integrated value), in which the transition induced in NH_3 is $\tilde{A}'\ A_2''$–$\tilde{X}'\ A_1$. The primary process and the quantum yield of each reaction involved in the resulting photodissociation will obviously depend on λ, as follows[19,21]:

1. In region 1, $112 < \lambda < 140$ nm, the primary processes are:

$$NH_3 + h\nu \Rightarrow NH(X^3\Sigma) + H + H \quad (3)$$

$$NH_3 + h\nu \Rightarrow NH^*(a^1\Delta) + H_2 \quad (4)$$

$$NH_3 + h\nu \Rightarrow NH^*(b^1\Sigma) + H + H \quad (5)$$

$$NH_3 + h\nu \Rightarrow NH^*(c^1\Pi) + H + H \quad (6)$$

2. In region 2, $140 < \lambda < 170$ nm, the observed primary processes are reaction (4) and

$$NH_3 + h\nu \Rightarrow NH_2^*(\tilde{A}^2 A_1) + H \quad (7)$$

3. Finally, in region 3, $170 < \lambda < 220$, reaction (4) and

$$NH_3 + h\nu \Rightarrow NH_2(\tilde{X}^2 B_1) + H \quad (8)$$

were observed.

The excited states of amino (NH_2) and imino (NH) radicals in the above-mentioned reactions are marked with an asterisk. Secondary reactions (not shown) include the recombination of hydrogen atoms, recombination of NH_2 with H (both leading to the disappearance of radicals), as well as the creation of stable molecules, N_2H_4 and N_2, through $NH_2 + NH_2$ and NH + NH reactions, respectively. Although the dissociation energy of amino and imino radicals is 4.1 and 3.5 eV, respectively, they absorb only in the UV/vis range, so that their photodissociation as a result of VUV irradiation can be neglected.[19,21]

Polyolefins like PE and PP are composed of only C—C and C—H bonds, and they possess the simplest absorption spectrum of all polymers[6–8] [see Fig. 2(a)]. The absorption starts to increase below 160 nm, increases to values of about 10^5 (for PE) and 3.4×10^5 (for PP) cm^{-1} near 120 nm, and peaks near 80–90 nm with a value about two or three times higher. The absorption leads to homolytic scission of C—C, and C—H bonds, followed by the formation of alkyl (–$CH_2C^*HCH_2$–) and allyl (–$CH_2C^*HCH{=}CHCH_2$–) radicals[9–11] on the polymer surface that can evidently undergo further reactions. On the outermost surface they can react with amino and imino radicals in the neighboring gas phase, thereby incorporating nitrogen-containing functional groups, which are chemically bonded to the polymer surface. In the region where gas molecules have no access, radicals can recombine among one another to form a linkage, or a radical can split a hydrogen atom from a neighboring carbon atom to form a double bond (C=C).[4,9,11,13] The generally accepted mechanism whereby new chemical species are incorporated onto polymer surfaces involves simultaneous activation (formation of free radicals) of both the solid and gas phases, followed by heterogeneous reaction of these chemically activated species. However, to date there is only scanty published evidence to support this proposed mechanism; generally speaking, chemical modification of polymer surfaces is a rather complex, not yet completely understood process, and in the present research we aim to provide additional clarification.

Using our various lamp emissions for polymer irradiation in low-pressure ammonia, three types of irradiation experiments were carried out (see Fig. 2 for details):

1. For the case of the Kr lamp ($\sim 85\%$ of the radiation is emitted in region 1), both ammonia molecules and the polymer surface were efficiently activated because of their high-absorption coefficients in this spectral range.

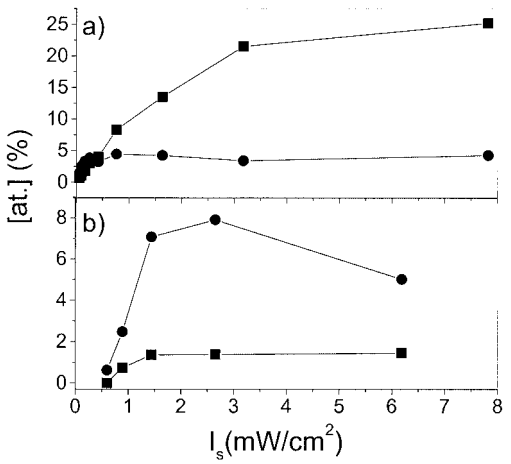

Figure 3 Surface concentrations (in at. %) of nitrogen [N] (■) and oxygen [O] (●), incorporated during irradiation of LDPE for 60 min in flowing NH_3 (p = 300 mTorr) with the Kr lamp (a) and the D_2Ar lamp (b), as a function of I_s.

2. In the case of the D_2Ar lamp (~ 75% of radiation is emitted in region 2), the polymer surface was efficiently activated, but not the gas phase; that is, only relatively small concentrations of NH and NH_2 radicals were formed, given that the absorption coefficient of NH_3 is low, resulting in low quantum yields for the NH_3 photodissociation reactions.
3. For the Xe excimer lamp, most of the radiation (~ 70% of the radiation is emitted in region 3) was absorbed only by NH_3 molecules, producing NH and NH_2 radicals that can possibly react with the unactivated polymer surface.

Therefore, it would appear possible to investigate the relative importance of contributions of surface and/or gas phase activation to the overall reaction using this set of experiments; this can then provide valuable information concerning the mechanisms involved in the photochemical surface modification.

In Figure 3 the evolutions of nitrogen [N] and oxygen [O] surface concentrations (determined by XPS) are plotted versus I_s for VUV-treated LDPE. Figure 3(a) and (b) pertain to irradiations using the Kr and the D_2Ar lamps, respectively, both for total durations of 60 min. Different I_s values were achieved by varying the frontal distance d between the lamp's MgF_2 window and the sample surface, based on eq. (1). It can be seen that by using the Kr lamp [Fig. 3(a)] we can obtain high [N] values (up to 25%), roughly proportional to I_s, until saturation is reached near 3 mW/cm^2. This can readily be explained by the fact that the radical concentration at the polymer surface ([R*]) is proportional to the photon flux; however, for high flux and [R*] values, the radicals react rapidly with one other, rather than with species in the gas phase. This leads to an increase in the concentration of C═C double bonds (i.e., creation of polyenyl $-CH_2C^*H(CH{=}CH)_nCH_2-$ type radicals)[9–11] at the expense of nitriding reactions. The presence of some oxygen ([O] ≤ 5%) can be attributed to reactions between long-lived radicals or unstable functional groups created during the VUV irradiation with molecular oxygen or water vapor when the samples were subsequently exposed to ambient atmosphere.[22] Regarding Figure 3(b), corresponding to D_2Ar irradiation, the situation is seen to be very different from Figure 3(a): although only 1.5 % [N] is incorporated into the LDPE surface, [O] is seen to increase to nearly 8%. This can be attributed to the relatively high degree of surface activation of the polymer, accompanied by inefficient photodissociation of NH_3 in the gas phase.[19,21]

Finally, regarding treatment 3, Xe excimer radiation (region 3), although similar experimental conditions were used, no measurable nitrogen incorporation was detected by XPS on LDPE. PE absorbs very little radiation with $\lambda > 160$ nm: its (low) absorption coefficient in this spectral range is attributed only to impurities, additives, and structural anomalies, such as C═C double bonds present in the polymer structure. Because the polymer we used was pure and additive-free, and contained only very few C═C bonds (below detectability by FTIR analysis of the untreated polymer), we indeed expected a very low level of surface activation during treatment 3. This, combined with the low reactivity of NH/NH_2 radicals[19,21] toward inactivated polymer surfaces, can explain why we found [N] ≈ 0.

To further investigate the role of polymer surface activation by VUV, we treated LDPE samples in the two different geometrical configurations shown in Figure 1(b):

1. In the first case, discussed so far in this article, the sample was oriented perpendicularly to the VUV source, and was thereby subjected to the combined exposure to VUV photons and to radicals in the gas phase.
2. In the second case, the sample surface was parallel to the flux of VUV photons, and was therefore subjected only to the action of free radicals created by the photons in the gas phase.

The results obtained with the Kr lamp in configuration 1 ("$\perp$ hν") [see Fig. 4(a)] show high [N] values, up to 25%, in agreement with our earlier results.[12] Interestingly, samples treated in the second configuration ("$\parallel$ hν") displayed [N] ≤ 10% (nearly half of the maximum value obtained in configuration 1), merely through the action of the gas-phase radicals; this result is somewhat surprising, considering the saturated and chemically rather inert polymeric surface. However,

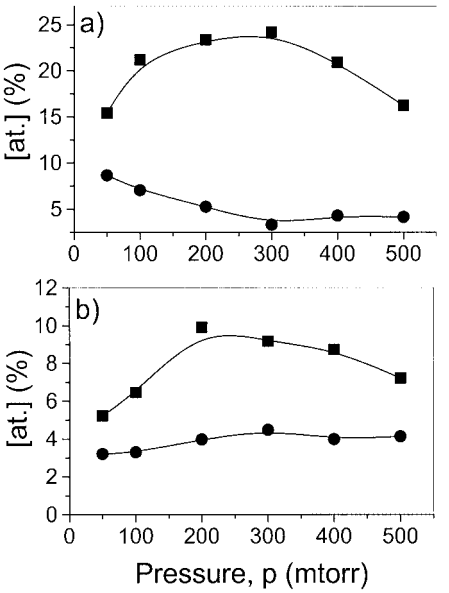

Figure 4 Surface concentrations (in at. %) of [N] (■) and [O] (●), for LDPE treated with the Kr lamp in flowing NH_3 (p = 300 mTorr) (a) perpendicular (⊥) and (b) parallel (∥) to the photon flux; treatment duration, t = 60 min, I_s = 7.82 mW/cm^2.

some of the imino radicals, that is, the NH* ($c^1\Pi$) state resulting from reaction (6), possessed sufficient energy (E = 5.37 eV) for bond scissions (the bond energies in polyolefins are 3.7 eV for C—C and 4.1–4.9 eV, for C—H).[7,8] They were then able to react with the polymer chains, leading to nitrogen incorporation. Furthermore, atomic hydrogen is also well known for its chemical reactivity and its ability to abstract hydrogen atoms from the polymer chain, thereby enabling reactions with NH/NH_2 radicals from the gas phase.

Based on the results we have presented so far, we therefore believe that VUV-induced chemical modification of polymer surfaces involves free-radical formation attributed to absorption of VUV photons and/or to energetic gas particles, followed by reactions of the radicals with activated species in the gas phase.

Figures 4(a) and 5 show [N] and [O] plotted as a function of NH_3 pressure p for LDPE and BOPP samples, respectively, when exposed to radiation from the Kr lamp. Both polyolefins show the same general features, that is, an initial increase in [N] with rising p, followed by a broad maximum and a decrease. The concentration of NH_x^* radicals in the gas phase is proportional to p (at relatively low pressures); however I_s, and consequently the surface concentration of radicals [R*], decays exponentially with increasing p [eq. (1)]. Because the extent of surface modification appears to be determined by activation of both the gas and solid phases, the two combined evolutions lead to the observed maximum.

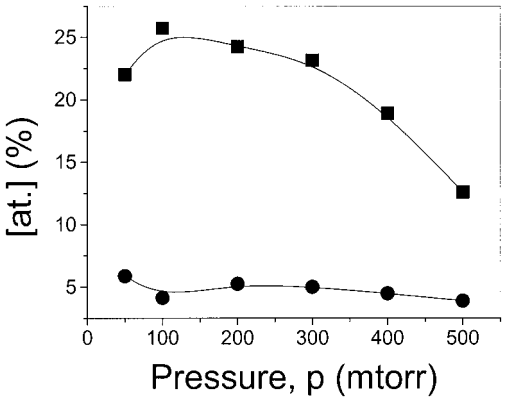

Figure 5 Surface concentrations (in at. %) of [N] (■) and [O] (●), as a function of NH_3 pressure, for BOPP treated with the Kr lamp; I_s = 7.82 mW/cm^2, t = 60 min.

In Figure 6 we plotted [N] and [O] as a function of treatment duration t (and energy density or dose E_d), again for the case of the Kr lamp, for LDPE [Fig. 6(a)] and BOPP [Fig. 6(b)]. We define R, the rate of surface modification, $R \equiv d[N]/dt$, by the slope of the near-linear increases after t = 0. Although [N] rises to similar maximum values (~ 25%) for both polymers, their R values are seen to be different: R = 4.6 ± 0.3 (% min^{-1}) for LDPE and R = 0.47 ± 0.03 (% min^{-1}) for BOPP. At saturation ([N] ≈ 25%), the polymer depth sampled by XPS (x ≈ 10 nm) contains one nitrogen functional group for each polymer repeat unit. Given

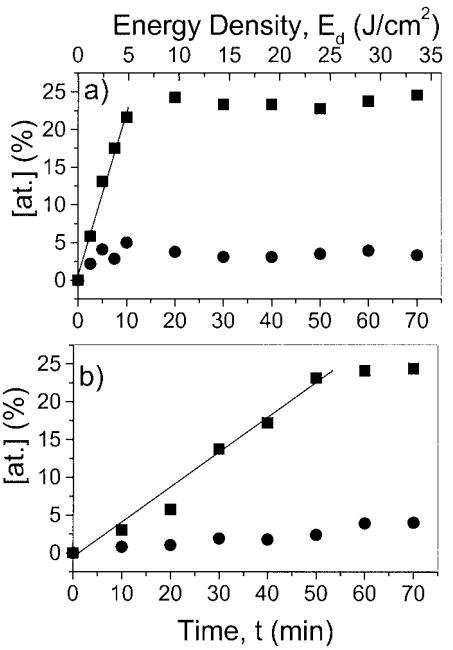

Figure 6 Dependency on irradiation time t of the surface concentrations of [N] (□) and [O] (●), for (a) LDPE and (b) BOPP treated with the Kr lamp; I_s = 7.82 mW/cm^2, p_{NH3} = 300 mTorr.

that great care was taken to ensure identical conditions throughout these experiments, the differences observed between LDPE and BOPP in Figure 6(a) and (b) must be attributed to the characteristics of these polymers themselves. We believe that the 10-fold lower *R* value of BOPP is attributable to this polymer's higher ablation (etch) rate under irradiation by 123.6 nm photons, resulting from cleavage of its pendant methyl groups. These observations are confirmed by the findings of Wilken et al.,[23,24] who reported that 75% of the overall VUV-induced changes are caused by polymer ablation and only 25% by structural modification (e.g., creation of C═C double bonds) for the case of PP, whereas for PE the corresponding values were 30 and 70%, respectively. In other words, BOPP ablates more rapidly than LDPE, and eventually attains the observed saturation value ([N] ≈ 25%), much more slowly, only after the surface is stabilized against the further ablation through structural changes such as crosslinking reactions.

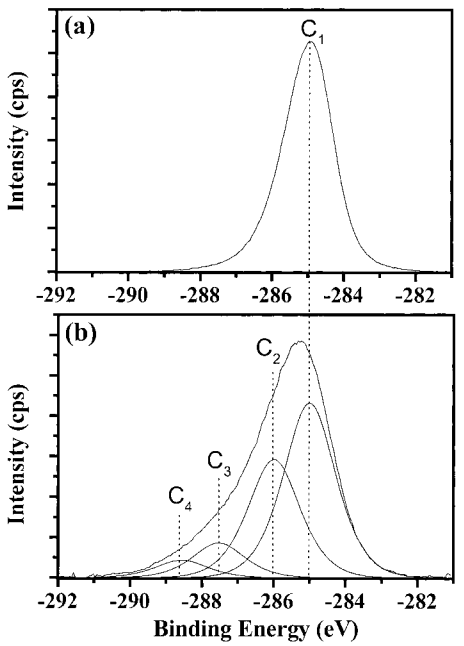

Figure 7 High-resolution Cls spectra of (a) virgin BOPP and (b) treated BOPP, irradiated with the Kr lamp; I_s = 7.82 mW/cm^2, p_{NH3} = 300 mTorr, t = 60 min (E_d = 28.2 J/cm^2).

Surface chemistry

In addition to providing the total heteroatom concentrations on the surfaces of VUV-treated LDPE and BOPP presented above, XPS was also used to characterize their chemical bonding states.

Untreated polyolefins exhibit a single high-resolution Cls peak at BE = 285.0 eV, which corresponds to C—C and C—H bonds [i.e., –CH, –CH_2, –CH_3 groups, Fig. 7(a)]. VUV treatment with the Kr lamp broadened the peak and introduced a tail at higher BE because of the incorporation of N atoms, which are chemically bonded to carbon. Because similar results were obtained for both polymers, we discuss only the spectrum of a BOPP sample (E_d = 28.15 J/cm^2) shown in Figure 7(b). The results of the Cls, Nls, and Ols high-resolution spectral deconvolutions and their assignments are presented in Table II. After treatment, the C_1 component of the Cls spectrum is almost unchanged, apart from slight broadening, FWHM = 1.7 eV (an increase by 0.1 eV), but the new component peaks include C_2–amine (C—N, 285.9 eV), C_3–carbonyl (C═O in aldehydes and ketones, 287.2 eV), and C_3–amides (N—C═O, 288.5 eV), the C—N peak being the dominant one.[25,26] Although attempts to explicitly include functionalities like C—O (at +1.5 eV) and C═N (at +1.7 eV) failed, we cannot exclude their possible presence solely on the basis of XPS results. However, ATR-FTIR results (see below) showed that hydroxyl, imine, and nitrile groups exist only in small concentrations, if they are at all present.

Deconvolution of the N1s and O1s peaks can be useful to confirm the Cls results. The N1s peak was resolved into two components, N_1 (399.0 eV) and N_2 (400.3 eV; see Table II) assigned to amines and amides, respectively. Unambiguous deconvolution of O1s peak was more difficult, the best fit (see Table II) again being used as an internal check of the Cls data. We obtained three component peaks, O═C—N at 531.3 eV, C═O at 532.3 eV, and O—C—O at 533.6 eV, the latter possibly indicating a small concentration of hydroxyl groups. Certain functional groups like oxime (C═NOH), nitro (–NO_2), and nitrate (C—ONO_2) can be excluded because no significant shift was observed in the N1s peak.[25,26]

Because the XPS analysis failed to give unambiguous results, as we just pointed out, we obtained complementary information from infrared spectroscopy. The ATR-FTIR spectra of untreated and treated LDPE are presented in Figure 8(a) and (b) (difference spectrum), respectively, whereas the corresponding results for BOPP are shown elsewhere.[12] Given that the sampling depth of the present ATR-FTIR technique (~ 0.5 μm) is large compared with the estimated depth of VUV treatment effects (a few tens of nanometers, depending on λ),[9,11] the signal coming from the modified surface is "diluted" by that of the polymer "bulk." To highlight the chemical changes in the surface, one must therefore subtract the spectrum of the untreated sample from the treated one; the difference spectrum of a 28.15 J/cm^2 NH_3/VUV-treated LDPE sample is presented in Figure 8(b), where the arrows identify the positions of new peaks. As we can see, the VUV treatment introduces three new IR bands, as follows:

1. A very broad band between 3550 and 3050 cm^{-1}, centered at about 3270 cm^{-1}, can be attributed to

TABLE II
High-Resolution XPS Cls, Nls, and Ols Peak Assignments for BOPP Treated with Kr Lamp[a]

Spectrum	Peak	Center (eV)	ΔBE (eV)	Assignment	% Area
C1s	1	285.0	0	C—C, C—H	56.66
	2	285.9	0.9	C—N	34.26
	3	287.2	2.2	C═O, C—O	10.05
	4	288.5	3.5	N—C═O, C—N—C ‖ ‖ O O	5.04
N1s	1	399.0	—	C—N	65.53
	2	400.3	—	N—C═O, C—N—C ‖ ‖ O O	34.47
O1s	1	531.3	—	N—C═O	53.13
	2	532.3	—	C═O	37.47
	3	533.6	—	O—C—O	9.4

[a] I_s = 7.82 mW/cm^2; E_d = 28.15 J/cm^2; NH_3, p = 300 mTorr; t = 60 min.

N—H stretch in primary (3460–3280 cm^{-1}) and secondary (3350–3300 cm^{-1}) amines, as well as N—H stretch in primary (3400–3380 cm^{-1}) and secondary (3300–3280 cm^{-1}) amides. We excluded from the assignment the O—H stretch in alcohols and phenols because we did not observe a band at about 1260–1000 cm^{-1}, characteristic of the strong C—OH stretch vibration in alcohols, nor the 720–600 cm^{-1} strong O—H out-of-plane vibration in phenols.

2. A broad band between 1750 and 1500 cm^{-1} has a doublet structure, subpeaks being centered at 1640 and 1560 cm^{-1}, respectively. This feature can be assigned to C═O stretch in aliphatic ketones (1725–1705 cm^{-1}), C═C and C═O in unsaturated ketones (1705–1665 cm^{-1}), C═O stretch in primary (1680–1660 cm^{-1}) and secondary (1680–1640 cm^{-1}) amides, NH_2 deformation in primary amines (1650–1590 cm^{-1}) and primary amides (1650–1610 cm^{-1}), as well as NH bending (1650–1530 cm^{-1}) in secondary amides. Some other possible groups in this region such as esters and carboxylic acids were eliminated because some of their characteristic strong vibrations were not found (i.e., the 1290–1180 very strong C—O—C antisymetric stretch in esters).
3. A relatively narrow band, between 1000 and 940 cm^{-1} with a peak at 960 cm^{-1}, can be assigned to CH out-of-plane deformation (1000–950 cm^{-1}), CH_2 out-of-plane wagging (950–900 cm^{-1}) in vinyl (–CH═CH_2), and CH out-of-plane deformation (980–955 cm^{-1}) in vinylene (–CH═CH–) with a high level of confidence.

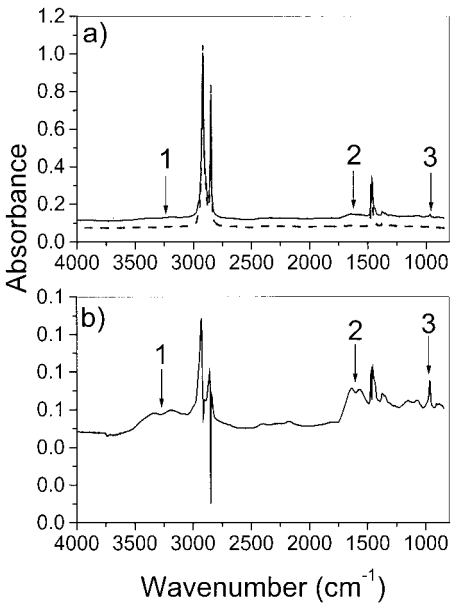

Figure 8 (a) ATR-FTIR spectra of untreated (dashed line) and treated (continuous line) LDPE, the latter with the Kr lamp, I_s = 7.82 mW/cm^2, p = 300 mTorr, t = 60 min (E_d = 28.2 J/cm^2); (b) difference spectrum/subtraction of the spectra in $(a)_0$ In both cases 200 spectra were added, at a resolution of 4 cm^{-1}.

These FTIR results are summarized in Table III, where certain possibilities (i.e., nitro groups) were already eliminated on the basis of XPS results. FTIR also confirmed that nitrogen forms only single bonds with carbon because we did not observe features near 2150–2100 cm^{-1} and 2240–2220 cm^{-1}, specific to imine C═N and nitrile C≡N groups, respectively.

We also performed ToF-SIMS analysis on the surfaces of both the untreated and treated polymers. The

TABLE III
Assignments of IR Absorbance Bands in the ATR-FTIR Difference Spectra of a Treated LDPE[a]

Wavenumber (cm^{-1})	Assignment
3270	NH stretch in primary/secondary amines and amides
1640	C═C, C═O stretch in amides, carbonyl (ketones and aldehydes), HN_2 deformations in primary amines
1560	HN_2 and NH deformations in amides, NH bend in secondary amides
960	CH out-of-plane deformation in vinyl and vinylene CH_2 out-of-plane wagging in vinyl

[a] Kr lamp, I_s = 7.82 mW/cm^2; E_d = 28.15 J/cm^2; NH_3, p = 300 mTorr; t = 60 min.

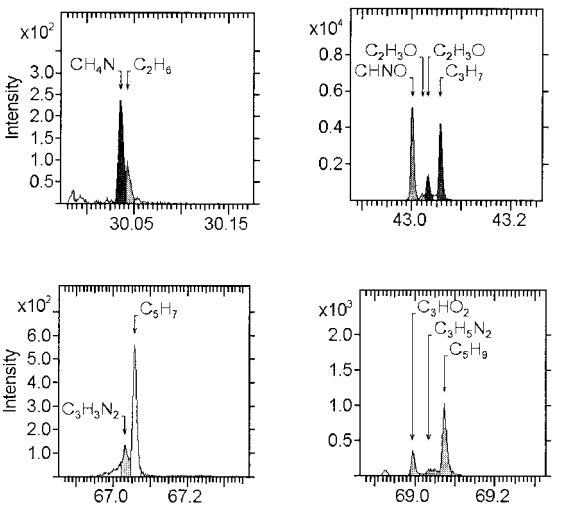

Figure 10 Some resolved components of peaks from Figure 9.

instrument's commercial software for peak assignments takes into account the differences between both measured and calculated mass values, as well as natural isotopic abundances. The results obtained for both our polyolefins are similar, whether treated or untreated. Therefore, we present here only those obtained for LDPE, for example, the positive ion scan of a NH_3/VUV-treated film (E_d = 14.07 J/cm^2; Fig. 9). The expected $C_xH_y^+$ fragments, characteristic of untreated PE, are quite evident, although closer inspection reveals certain new fragments, some of which are presented in Figure 10. We can identify three types of ions: (1) those containing only N, such as NH_3^+, CH_3N^+, CH_4N^+, $C_2H_3N^+$, . . . (at m/z = 17, 29, 30, 41, . . . , respectively) originating from amino groups; (2) those containing both O and N, such as $CHNO^+$, C_2HNO^+, $C_3H_6NO^+$ . . . (at m/z = 43, 55, 72, . . .) presumably coming from amides; and (3) those containing only O, such as CHO^+, CH_3O^+, $C_2H_3O^+$, . . . (at m/z = 29, 31, 43, . . .), which can be attributed to carbonyl groups in ketones and aldehydes. The dominant features at m/z = 73 and 148 in Figure 9 correspond to $C_3H_7NO^+$ and $C_5H_{12}N_2O_3^+$, respectively. Similar observations can also be made for the negative ion spectrum (Fig. 11), where we have identified (1) NH^-, NH_2^-, CN^-, CHN^-, . . . (at m/z = 15, 16, 26, 27, . . .); (2) NO^-, CNO^- (at m/z = 30,

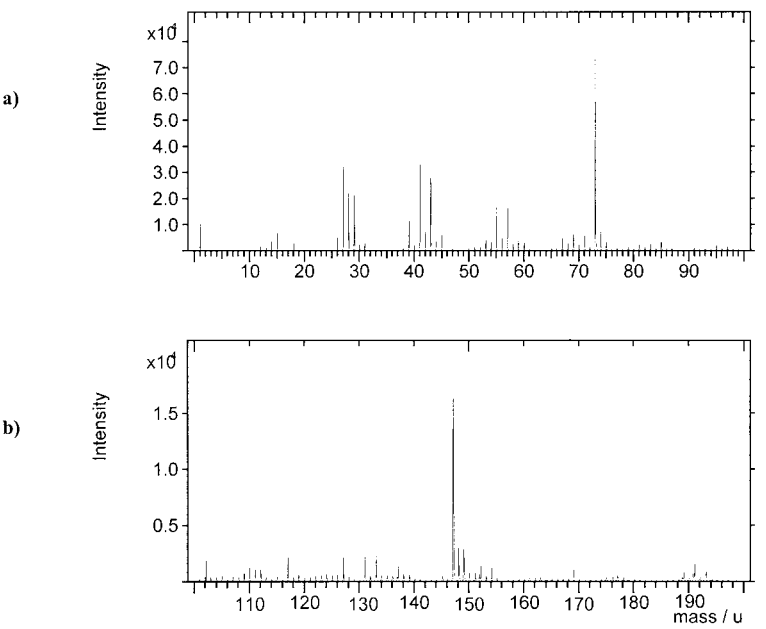

Figure 9 Positive ion ToF-SIMS spectrum for LDPE, VUV treated with the Kr lamp in flowing NH_3 at 300 mTorr (E_d = 14 J/cm^2); m/z = 0–200 range.

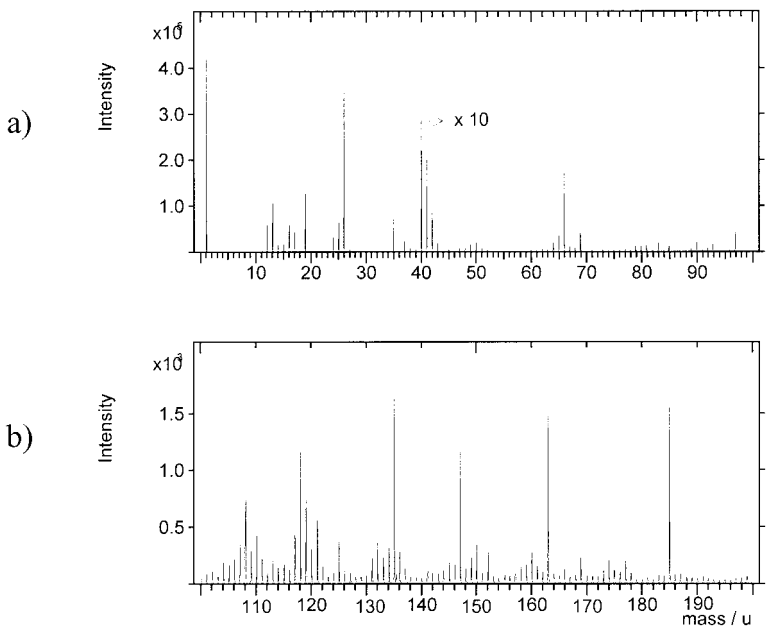

Figure 11 Negative ion ToF-SIMS spectrum for LDPE, VUV treated with the Kr lamp in flowing NH_3 at 300 mTorr (E_d = 14 J/cm^2); m/z = 0–200 range.

42); and (3) O^-, OH^-, CH_3O^-, $C_2H_3O^-$, . . . (at m/z = 16, 17, 31, 43, . . .) (see Fig. 12 for some examples). In fact, ions with the general structure $C_xH_yO_z/N_v^-$ are seen to dominate the negative ion scan up to m/z = 400 (e.g., $C_4H_2O^-$, m/z = 66); however, given that components increasingly overlap at higher mass, definitive peak assignments become more uncertain. The presence of heavier clusters containing N and/or O can also be attributed to the creation of unsaturations[26] and/or of LMWOM.[27]

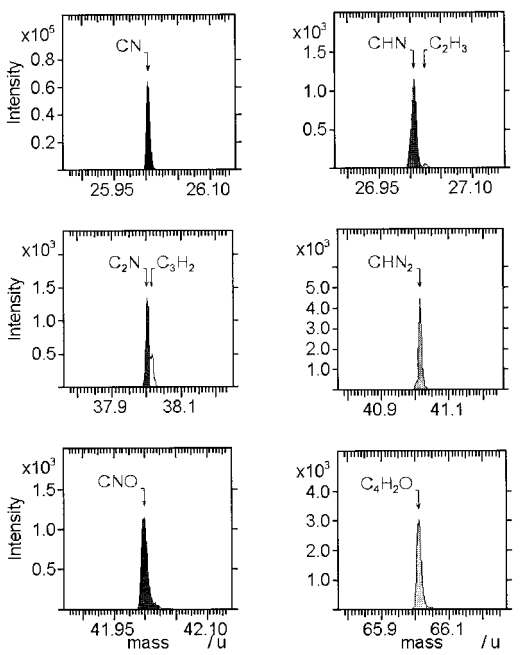

Figure 12 Some resolved components of peaks from Figure 11.

To summarize, based on the three complementary surface analysis techniques presented here (XPS, ATR-FTIR, and ToF-SIMS), we conclude that nitrogen is singly bonded to carbon, predominantly in primary and secondary amines, whereas the oxygen seems to form primarily double bonds with carbon, in carbonyl groups (amides, aldehydes, and ketones). Some unsaturations (C═C, in vinyl and vinylene groups) are also evident on the treated polymer surfaces, in agreement with expectations and with other results reported in the literature.[9,11,20,23,24]

Surface energy and topography

In Figures 13(a) and 14(a) we again show [N] and [O] (see also Fig. 6) as a function of E_d, before and after rinsing the samples in deionized water (full and open symbols, respectively), for LDPE and BOPP, respectively. For the same two polymers. Figures 13(b) and 14(b) show plots of the total surface energy γ_s and of its polar (γ_s^p) and dispersive (γ_s^d) components,[17,18] before and after rinsing, where

$$\gamma_s = \gamma_s^p + \gamma_s^d \ (\mathrm{mN/m}) \tag{9}$$

Note that all samples were treated with the Kr lamp under identical conditions (NH_3, p = 300 mTorr).

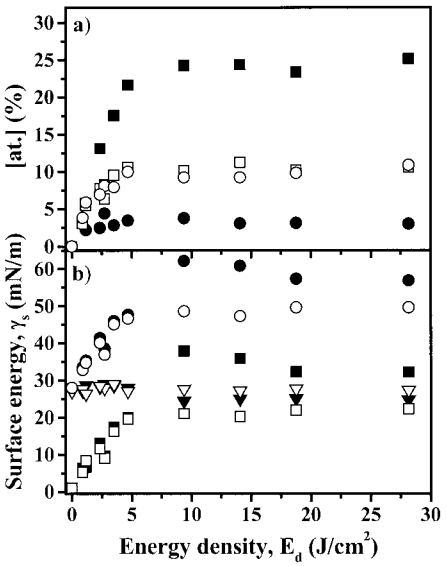

Figure 13 (a) Surface concentrations and (b) surface energy γ_s, as a function of the energy dose E_d, for NH_3 VUV-treated LDPE. (a) Surface concentration of nitrogen [N] (■) and oxygen [O] (●). (b) Surface energy γ_s (●) and its polar γ_s^p (■) and dispersive γ_s^d (▼) components. Open symbols pertain to the rinsed samples.

Comparing γ_s variations with E_d for the two polymers, we note the following:

1. γ_s tends toward asymptotic maximum values at approximately the same E_d values at which [N] have reached their own asymptotic limits.

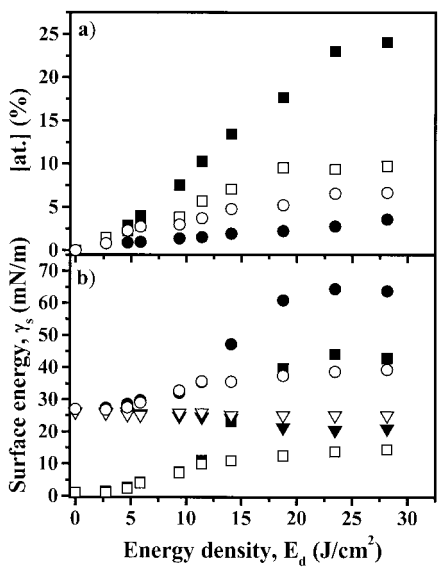

Figure 14 Surface concentrations and surface energy γ_s, as a function of the energy dose E_d, for NH_3 VUV-treated BOPP. (a) Surface concentration of nitrogen [N] (■) and oxygen [O] (●). (b) Surface energy γ_s (●) and its polar γ_s^p (■) and dispersive γ_s^d (▼), components. Open symbols pertain to the rinsed samples.

TABLE IV
[N], [O], and Surface Energy (γ_s) Measurements and Threshold for Appearance of "LMWOM" E_d^*

Polymer	[N] (%)	[O] (%)	[N]* (%)	[O]* (%)	γ_s^{max} (mN/m)	γ_s^{max*} (mN/m)	E_d^* (J/cm^2)
BOPP	25	4	10	7	65	40	5.5
LDPE	25	4	11	10	60	50	2.5

[a] Asterisks refer to samples after rinsing (Kr lamp, NH_3, p = 300 mTorr).

2. These E_d values are near 10 and 20 J/cm^2 for LDPE and BOPP, respectively, but γ_s^{max} appears to be slightly higher for the latter material (65 mN/m versus 60 mN/m for LDPE).

In Table IV we have summarized the most important results from Figures 13 and 14, both before and after rinsing.

Because γ_s^d remains practically constant with increasing E_d for both polymers, the observed increase in γ_s is entirely attributed to that of γ_s^p, consistent with the incorporation of new polar moieties in the polymer surface, as already shown in a previous section and elsewhere.[2,12,28] After rinsing in water, we noted significant decreases in [N] for both polymers, presumably because LMWOM is removed (see Table IV). Interestingly, [O] was seen to increase in both cases, which may be the result of the oxidation of long-lived radicals or to some other mechanisms under investigation. However, γ_s was seen to decrease, following the same trend as [N]; this suggests that the increase in [O] occurs beneath the polymer surface, within a depth that is inferior to that sampled by XPS (~ 10 nm, in our case), but that exceeds that "felt" by the sessile liquid drops (<1 nm). After rinsing, LDPE was seen to present a higher γ_s value than that of BOPP (50 and 40 mN/m, respectively), even though their [N]* values were similar. This is probably because of the higher propensity of BOPP toward degradation, as reflected by its relatively low "LMWOM threshold" value, E_d^* = 2.5 J/cm^2 (compared with 5.5 J/cm^2, for LDPE; see Table IV). For $E_d > E_d^*$, chain reactions dominate, giving rise to LMWOM formation, but to little or no additional N-incorporation onto the molecular chains.

Several authors have observed LMWOM to agglomerate as "nodules" on the surfaces of polymers (e.g., BOPP) during the following types of treatments: corona,[2,3,27] low-pressure plasma in oxygen,[13] atmospheric pressure glow discharge in nitrogen,[2] and ultraviolet/ozone.[16] To the best of our knowledge, there are no reports in the literature dealing with possible LMWOM formation on VUV-treated polymers, other than ablation studies.[4,23,24] Given that the data just

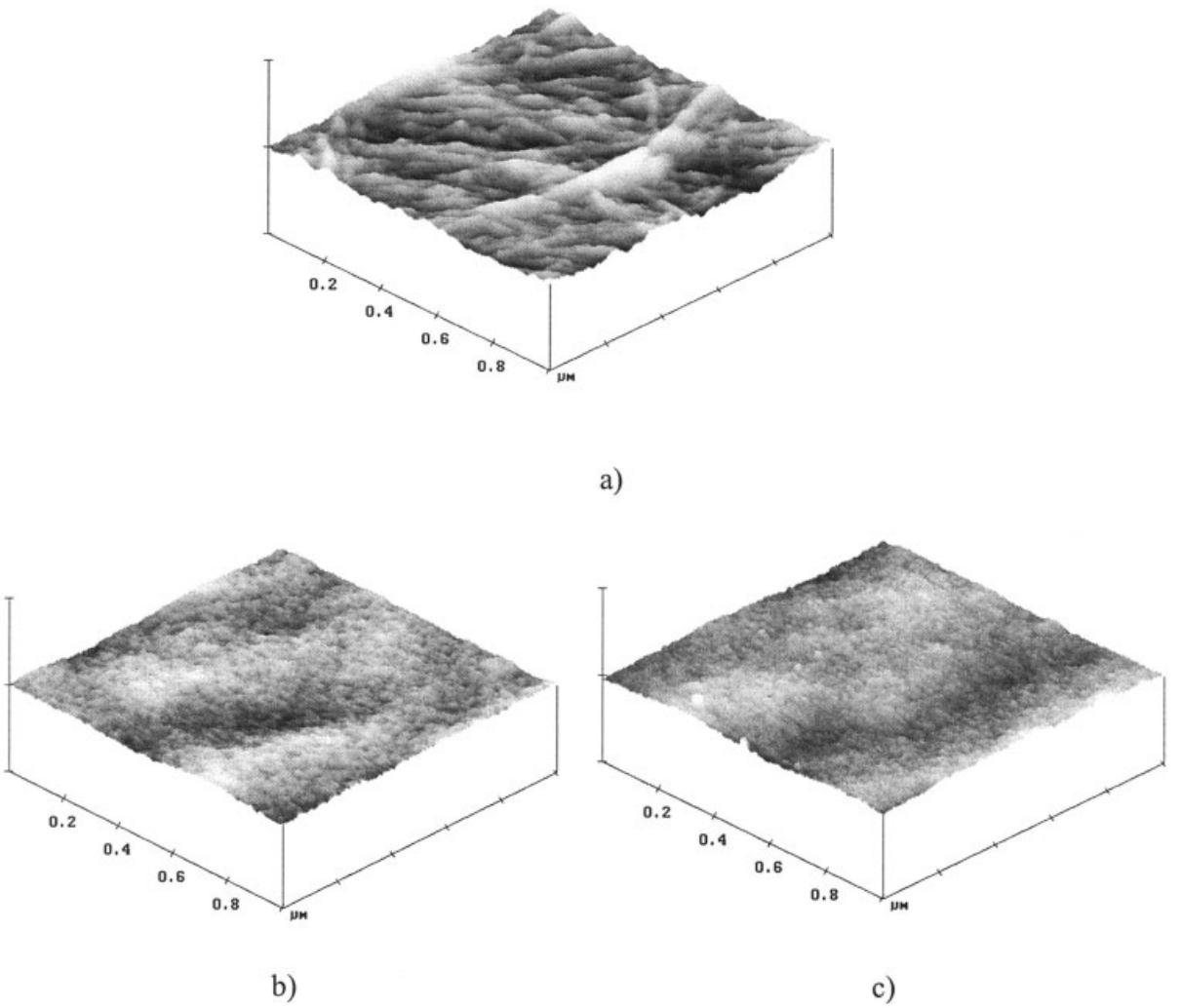

Figure 15 AFM images of BOPP surfaces: (a) untreated; (b) VUV-treated in flowing NH_3 at p_{NH3} = 300 mTorr (E_d = 28.2 J/cm^2); (c) VUV-treated (E_d = 28.2 J/cm^2), but rinsed in water; the vertical full scale is 30 nm for VUV-treated samples, and 100 nm for the untreated sample.

presented clearly suggest the removal of degraded material by rinsing treated samples in water (similar to the above-mentioned plasma treatments), we investigated the samples' surface topography. In Figure 15(b) we present an AFM image of a NH_3/VUV-treated (E_d = 28.2 J/cm^2) BOPP surface, whereas the same surface after washing is presented Figure 15(c). For comparison, Figure 15(a) shows the characteristic fine fibrillar structure of untreated BOPP, fibril diameters typically being $<$10 nm.[2,16,27] These fibrillar surface features are formed by bidirectional stretching of the polymer during the manufacturing process. For each case represented by Figure 15(a)–(c), at least five AFM images were taken randomly across the surface to ascertain that those presented here are representative.

Compared with the virgin BOPP, the VUV-treated surface was seen to be very smooth, even when examined on a more highly resolved z-axis scale (30 versus 100 nm for the untreated surface): the structure of the original BOPP surface is completely obliterated, suggesting destruction of the fibrils. This might be explained by preferential etching of the amorphous over the crystalline phase[4,29–31] attributed to higher mobility of the macromolecules in the former.[29,30] This, combined with crosslinking reactions, results in the observed progressively more uniform morphology over the entire surface.[30,31] Interestingly, no difference was observed in the surface structure after rinsing [compare Fig. 15(b) and (c)]; despite all earlier indications about degradation, AFM images show no evidence of "LMWOM" agglomeration on the VUV-treated surfaces. This may indicate that the degraded material is partially crosslinked, thereby being impaired from accumulating as "nodules." Rinsing the sample in water removes this loosely bonded "skin," which is uniformly spread over the surface of the otherwise undamaged polymer.

CONCLUSIONS

VUV irradiation in ammonia leads to the incorporation of chemically bonded nitrogen on polyolefin surfaces (LDPE and BOPP), accompanied by a considerable increase in the surface free energy of the treated samples. The mechanism of chemical modification apparently involves simultaneous activation of both the solid surface and of the gaseous ammonia, followed by a synergetic reaction of the resulting free radicals. We have shown that nitrogen is predominantly bonded in amines, but some oxygen is inevitably present in the form of carbonyl groups; other moieties, like hydroxyl groups, are either absent or in negligible concentrations. Unfortunately, VUV treatments can apparently damage the polymer surfaces, resulting in significant changes in their physicochemical properties (chemical composition and surface energy) after rinsing in water. However, the VUV-treated surfaces appear to be very smooth and display no evidence of LMWOM agglomeration as "nodules." VUV photochemically nitrided polymer surfaces are very distinct from their plasma-modified counterparts: the higher [N] concentrations of the former and their better-defined (amine-rich) surface characteristics may be advantageous for certain applications, for example, in the biomaterials field.

This work was supported by grants from the Natural Sciences and Engineering Research Council of Canada (NSERC). One of us (F.T.-M.) is grateful to the government of Quebec (Ministère de l'Éducation) for a postgraduate "bourse d'excellence." The authors are grateful to Gilles Jalbert for his skilled technical support and to Sebastien Guimond for the AFM images and for valuable discussions.

References

1. Mittal, K. L., Ed. Polymer Surface Modification: Relevance to Adhesion; VSP: Utrecht, 1996.
2. Guimond, S.; Radu, I.; Czeremuszkin, G.; Carlsson, D.J.; Wertheimer, M.R. Plasmas Polym 2002, 7, 71.
3. Strobel, M.; Dunatov, C.; Strobel, J. M.; Lyons, C. S.; Perron, J. S.; Morgen, M. C. Adhes Sci Technol 1989, 3, 321.
4. Fozza, A. C.; Klemberg-Sapieha, J. E.; Wertheimer, M. R. Plasmas Polym 1999, 4, 183.
5. Fozza, A. C.; Moisan, M.; Wertheimer, M. R. J Appl Phys 2000, 88, 20.
6. Onari, S. J Phys Soc Jpn 1969, 26, 500.
7. Partridge, R. H. J Chem Phys 1966, 45, 1685.
8. Partridge, R. H. J Chem Phys 1968, 49, 3656.
9. Skurat, V. E.; Dorofeev, Y. Angew Makromol Chem 1994, 216, 205.
10. Kuzuya, M.; Yamashiro, T.; Kondo, S.; Sugito, M.; Mouri, M. Macromolecules 1998, 31, 3225.
11. Wilken, R.; Holländer, A.; Behnisch, J. Surf Coat Technol 1999, 116–119, 991.
12. Truica-Marasescu, F.; Guimond, S.; Wertheimer, M. R. Nucl Instrum Methods Phys Res B, to appear.
13. Holländer, A.; Klemberg-Sapieha, J. E.; Wertheimer, M. R. J Polym Sci A 1995, 33, 2013.
14. Hudis, M.; Prescott, L. E. Polym Lett 1972, 10, 179.
15. Esrom, H.; Kogelschatz, U. Thin Solid Films 1992, 218, 231.
16. Nie, H. Y.; Walzak, M. J.; McIntyre, N. S. In: Polymer Surface Modification: Relevance to Adhesion; Mittal, K. L., Ed.; VSP: Utrecht, 2000; p. 377.
17. Kaelble, D. H. Physical Chemistry of Adhesion; Wiley: New York, 1971.
18. Owens, D. K.; Wendt, R. C. J Appl Polym Sci 1969, 13, 1741.
19. Okabe, H. Photochemistry of Small Molecules; Wiley: New York, 1978.
20. Holländer, A.; Wertheimer, M. R. J Vac Sci Technol A 1994, 12, 879.
21. Herzberg, G. Molecular Spectra and Molecular Structure, III: Electronic Spectra and Electronic Structure of Polyatomic Molecules; Van Nostrand: Princeton, NJ, 1966.
22. Klemberg-Sapieha, J. E.; Küttel, O. M.; Martinu, L.; Wertheimer, M. R. J Vac Sci Technol A, 1991, 9, 2975.
23. Wilken, R.; Holländer, A.; Behnisch, J. Plasmas Polym 1998, 3, 165.
24. Wilken, R.; Holländer, A.; Behnisch, J. Plasmas Polym 2002, 7, 185.
25. Beamson, G.; Briggs, D. High Resolution XPS of Organic Polymers: The Scienta ESCA 300 Database; Wiley: Chichester, UK, 1992.
26. Briggs, D. Surface Analysis of Polymers by XPS and Static SIMS; Cambridge University Press: Cambridge, UK, 1998.
27. Boyd, R. D.; Kenwright, A. M.; Badyal, J. P. S.; Briggs, D. Macromolecules 1997, 30, 5429.
28. Poncin-Epaillard, F.; Chang, Y. I. Langmuir 2000, 16, 1450.
29. Rabek, J. F. Photodegradation of Polymers: Physical Characteristics and Applications; Springer-Verlag: Berlin, 1996.
30. Poncin-Epaillard, F.; Brosse, J. C.; Falher, T. Macromolecules 1997, 30, 4415.
31. Herbert, S.; Shinozaki, D. M.; Collacott, R. J. J Mater Sci 1996, 31, 4655.